Antisense oligonucleotide-based therapeutic strategy for progranulin-deficient frontotemporal dementia

Geetika Aggarwal[1,2,3,10], Subhashis Banerjee[1,2,3,10], Spencer A. Jones[1,2,3], Monica Pavlack[2,3], Yousri Benchaar[4], Jasmine Bélanger[4], Myriam Sévigny[4], Denise M. Smith[1,2,3], Michael L. Niehoff[1,5], Ian Mitchelle S. de Vera[2,3], Terri L. Petkau[6], Blair R. Leavitt[6,7,8], Karen Ling[9], Paymaan Jafar-Nejad[9], Frank Rigo[9], John E. Morley[1], Susan A. Farr[1,2,3,5], Paul A. Dutchak[4], Chantelle F. Sephton[4], and Andrew D. Nguyen[1,2,3,*]

[1]Division of Geriatric Medicine, Department of Internal Medicine, Saint Louis University School of Medicine, St. Louis, MO, USA
[2]Department of Pharmacology and Physiology, Saint Louis University School of Medicine, St. Louis, MO, USA
[3]Henry and Amelia Nasrallah Center for Neuroscience, Saint Louis University, St. Louis, MO, USA
[4]Department of Psychiatry and Neuroscience, CERVO Brain Research Centre, Laval University, Quebec City, Quebec, Canada
[5]Veterans Affairs Medical Center, St. Louis, MO, USA
[6]Centre for Molecular Medicine & Therapeutics, Department of Medical Genetics, University of British Columbia, B.C. Children's Hospital, Vancouver, BC, Canada
[7]Division of Neurology, Department of Medicine, University of British Columbia Hospital, Vancouver, BC, Canada
[8]Center for Brain Health, University of British Columbia, Vancouver, BC, Canada
[9]Ionis Pharmaceuticals, Carlsbad, CA, USA
[10]These authors contributed equally
*Correspondence: andy.d.nguyen@health.slu.edu

ABSTRACT

Loss-of-function *GRN* mutations result in progranulin haploinsufficiency and are a common cause of frontotemporal dementia (FTD).[1,2] Antisense oligonucleotides (ASOs) are emerging as a promising therapeutic modality for neurological diseases,[3,4] but ASO-based strategies for increasing target protein levels are still relatively limited. Here, we report the use of ASOs to increase progranulin protein levels by targeting the miR-29b binding site in the 3' UTR of the *GRN* mRNA, resulting in increased translation.

INTRODUCTION

Progranulin is a lysosomal and secreted protein with pleiotropic effects, including promoting neuronal survival, neurite outgrowth, wound healing, tumor cell growth, and modulating inflammation.[5,6] Haploinsufficiency of progranulin causes frontotemporal dementia (FTD),[1,2] and thus increasing progranulin levels is a clear therapeutic goal.[7,8] Gene therapy studies in mice provide proof of concept that restoring progranulin levels in heterozygous *Grn* mice improves FTD-associated neuropathology and behavioral deficits.[9] However, there are currently no approved therapies that increase progranulin levels for progranulin-deficient FTD.

Antisense oligonucleotides (ASOs) are emerging as a promising therapeutic modality for neurological diseases,[3,4] but ASO-based strategies for increasing target protein levels are still relatively limited. ASOs are short synthetic oligonucleotides that can be used to modulate target RNAs. The most commonly used ASO strategies involve RNase H1-mediated degradation of the target mRNA and modulation of splicing of the target mRNA.[3] Several strategies have been described for increasing target protein levels, including targeting upstream ORFs (uORFs)[10] and regulatory elements in the 5' UTR.[11] However, these approaches are limited by the fact that not all genes possess uORFs and/or 5' regulatory elements.

Levels of approximately 30-60% of all human proteins are regulated by microRNAs (miRs).[12,13] These miRs typically bind to the 3' UTR of target mRNAs and decrease protein levels through translational repression or mRNA decay.[14] In the current study, we investigated if ASOs targeting the miR-29b binding site[15] in the 3' UTR of the human *GRN* mRNA can effectively increase progranulin protein levels.

RESULTS AND DISCUSSION

Three miRs, including miR-29b, have been reported to regulate progranulin protein levels.[15-19] Consistent with previous reports,[15,16] treatment with a broad miR-29b inhibitor increased progranulin protein levels (Figure 1a) in H4 neuroglioma cells, which have moderate expression of miR-29b (Supplementary Figure S1a). Data from the Human miRNA Tissue Atlas[20] show that miR-29b is expressed in the human brain (Supplementary Figure S1b). To test if ASOs targeting the miR-29b binding site can increase progranulin protein levels, we designed a panel of 18-mer ASOs with 2'-*O*-methoxyethyl (MOE) ribose- and phosphorothioate-modifications that span the

entire miR-29b binding site with single nucleotide resolution (Figure 1b). Our initial ELISA-based screening in H4 cells at 5 μM identified 11 ASOs that increased progranulin protein levels by >15% (Supplementary Figure S2). We subsequently validated these 11 ASOs (M1, M2, M3, M5, M6, M10, M11, M31, M36, M38, M39) and identified 5 additional ASOs (M4, M25, M28, M29, M40) that increased progranulin protein levels at 10 μM ASO, as determined by western blot (Figure 1c). Because progranulin is also secreted from cells, we tested if the ASOs similarly increased levels of progranulin in the conditioned media. We found that ASOs that increased cellular progranulin levels also increased secreted progranulin levels (Supplementary Figure S3), suggesting the observed increases in cellular progranulin levels are not due to altered trafficking or secretion.

Time course studies determined that increased progranulin levels are detectable within 1–2 h of ASO treatment for M6 and M10, and by 8 h for M36 (Supplementary Figure S4). Dose curve experiments show the ASOs exhibit dose-dependent effects with EC_{50} values in the range of 1–8 μM (Figure 1d and Supplementary Figure S5). These ASOs exhibited no detectable toxicity in H4 cells, as determined by MTT assay (Supplementary Figure S6). We next tested select ASOs in iPSC-derived neurons[21] and found these ASOs similarly increased progranulin protein levels in a dose-dependent manner (Figure 1e). To test the ASOs *in vivo*, we used a recently developed humanized *GRN* mouse model;[22] intra-striatal injection of a miR-29b inhibitor was previously shown to increase progranulin protein levels in the brains of these mice.[22] At three weeks following intracerebroventricular (ICV) administration of 500 μg ASO,[23] we observed increased human progranulin protein by ELISA in the cortex of mice that received ASO M5 (Figure 1f). Progranulin levels were increased by 53% and 55% in male and female mice, respectively, compared to mice of the same sex that received the scrambled control ASO. By western blot, we also observed increased human progranulin levels in the thalamus and hippocampus of mice that received ASO M5 (Figure 1g). Together, these results demonstrate that ASOs targeting the miR-29b binding site can increase human progranulin protein levels in cells and *in vivo*.

Despite increasing progranulin protein levels, most of the ASOs did not increase *GRN* mRNA levels in H4 cells (Figure 2a), suggesting that the ASOs increase the rate of progranulin translation. This would be consistent with the canonical effects of translational repression by many miRs.[14,24] To formally test this, we performed ribosomal profiling experiments to assess the amount of ribosome-bound *GRN* mRNA, which reflects its rate of translation. We found that cells treated with ASOs M10 and M36 had a marked enrichment of *GRN* mRNA in the heavy polyribosome fractions (11–16), compared to cells treated with a scrambled control ASO (Figure 2b), strongly suggesting that the ASOs increase the rate of progranulin translation. To determine if the ASOs increase the amount of newly synthesized progranulin protein, we used the methionine analog azidohomoalanine (AHA) to label nascent proteins. Following immunoprecipitation of progranulin, western blots using fluorescently labeled-streptavidin confirmed that ASOs M5, M10, and M36 increased the synthesis of progranulin protein (Figure 2c). We next tested if the ASOs act through miR-29b by using a miR-29b inhibitor. The experiments of Figure 2d demonstrate that ASOs M5 and M10 increased progranulin levels similarly to the miR-29b inhibitor and importantly that the miR-29b inhibitor abrogated any further effects of the ASOs on progranulin levels, strongly suggesting that the ASOs block miR-

29b's effect on progranulin. Lastly, we performed a FRET-based assay to test if the ASOs compete for binding of miR-29b to a partial *GRN* 3' UTR RNA containing the miR-29b binding site *in vitro*. We found that ASOs M29, M31, and M36 were able to effectively compete off miR-29b binding (Figure 2e), with IC_{50} values in the range of 0.4–0.8 µM. The scrambled control ASO and several ASOs which do not overlap with the binding site (i.e., M2 and M5) were unable to displace miR-29b; it is possible the partial *GRN* 3' UTR RNA used in this assay does not completely recapitulate aspects of the full length *GRN* mRNA, such as secondary structure. Nonetheless, these ASOs increase translation of progranulin protein in intact cells in a miR-29b-dependent manner (Figure 2b-d).

Together, these studies establish the mechanism of action is that these ASOs displace miR-29b from its binding site and thereby de-repress translation, resulting in increased progranulin protein levels. While our current study focuses on ASOs that target the miR-29b binding site, we have also tested a smaller panel of ASOs targeting the miR-659 binding site[17,18] in the *GRN* 3' UTR (see Figure 1b) and identified ASOs that similarly increase progranulin protein levels (Supplementary Figure S7). Future studies will focus on testing if the ASOs can delay or prevent the progression of FTD-associated neuropathology and behavioral deficits in mouse models.

To our knowledge, this is the first in-depth characterization of using ASOs to increase translation of a target protein by sterically blocking a miR binding site. Two previous studies used oligonucleotides to block miR binding sites,[25,26] but these reports lacked details about the targeting strategy and/or the mechanism of action. Our results suggest that this ASO strategy may be broadly applicable for pharmacologically increasing levels of target proteins and could be particularly useful for development of ASO-based therapies for diseases of haploinsufficiency.

MATERIALS AND METHODS

ASOs – ASOs used in these studies were 18-mer ASOs uniformly modified with 2'-*O*-methoxyethyl (MOE) sugars with a phosphorothioate backbone, with the following exceptions: ASOs used in the experiment shown in **Supplementary Fig. 7** were modified with 2'-*O*-methyl sugars with a full phosphorothioate backbone, and ASOs M5 and M6 in **Fig. 1f** were modified with MOE with a mixed phosphorothioate backbone. ASOs used for in vitro and cell-based studies were dissolved in water and stored at -20 °C. For in vivo studies, lyophilized ASOs were dissolved in sterile PBS without calcium or magnesium (Gibco, 14190-250), and sterilized by passing through a 0.2 µm filter. The miR-29b inhibitor is a 23-mer ASO containing uniform 2'-MOE sugar and phosphorothioate backbone modifications.

Cell culture – H4 human neuroglioma cells were obtained from ATCC (HTB-148) and cultured in DMEM (Dulbecco's Modified Eagle Medium, high-glucose) (Gibco, 11995-073) supplemented with 10% fetal bovine serum (FBS) (Gibco, 26140-095), 10 U/ml penicillin, and 10 µg/ml of streptomycin. For typical ASO treatments, cells were plated in 6-well or 12-well plates, and then treated with ASOs as indicated on the following day. Human iPSCs harboring doxycycline-responsive Neurogenin -2 (NGN2) expression for differentiation into i3 cortical neurons were

kindly provided by Michael Ward. Cells were grown and differentiated as described.[20] After 2 weeks of differentiation, i3 neurons were treated with ASOs for 3–4 days. All cells were maintained at 37 °C and 5% CO_2.

ELISA and immunoblot analysis – For progranulin measurements, cells were rinsed with PBS and then lysed in RIPA buffer containing protease inhibitors (Roche, cOmplete Mini EDTA-free Protease Inhibitor Cocktail). Cleared lysates were transferred to new tubes, and protein concentrations were determined using the Bio-Rad DC Protein Assay Kit II. For ELISA, progranulin concentrations were determined in duplicate using 10–15 µl of lysates per well (typically 8–20 µg of total protein per well) using a sandwich ELISA assay (R&D Systems, DPGRN0). For experiments analyzing secreted progranulin, conditioned media was collected and cleared at 10,000 x g for 10 min at 4° C. For western blot analysis, sample buffer was added to the lysates or conditioned media, and the samples were heated at 95 °C for 10 min. Equal amounts of protein lysates (10–20 µg) or equal volumes of conditioned media (10–20 µl) were separated on SDS–PAGE gels. Proteins were transferred to nitrocellulose membranes using the Bio-Rad Turbo-Blot transfer system. After blocking and antibody incubations, membranes were incubated with SuperSignal West Pico or Femto enhanced chemiluminescent HRP substrate (ThermoFisher) and visualized using a Chemi-Doc system (Bio-Rad). Primary antibodies used for immunoblot analysis were an anti-human progranulin linker 5 polyclonal antibody #614 that recognizes an epitope between amino acids 497–515,[27] and an anti-human vinculin monoclonal antibody (Cell Signaling Technology, 13901). The secondary antibody used was HRP-conjugated AffiniPure goat anti-rabbit IgG (H+L) (Jackson Immuno Research Labs, 111-035-144).

RNA analysis – Total RNA was isolated from cultured cells using the RNeasy Mini kit (Qiagen, 74106) with on-column DNase digestion (Qiagen, 79256). RNA was reverse-transcribed to obtain cDNA using the iScript cDNA synthesis kit (Bio-Rad, 1708891), and qPCR was performed using PowerUp SYBR Green Master Mix (ThermoFisher, A25777) with a Bio-Rad CFX384 Real-Time System. Primers sequences were as follows: human CYCLO-F, GGAGATGGCACAGGAGGAAA; human CYCLO-R, CCGTAGTGCTTCAGTTTGAAGTTCT; human GRN-F, AGGAGAACGCTACCACGGA; and human GRN-R, GGCAGCAGGTATAGCCATCTG. Results for qPCR were normalized to the housekeeping gene CYCLO and evaluated by the comparative C_T method. For RNA-seq analysis of miR levels, the small RNA fraction was isolated from triplicate 100-mm dishes of H4 cells using the mirVana miRNA Isolation Kit (Invitrogen, AM1561). Libraries were constructed using the Ion Total RNA-Seq Kit v2 (Life Technologies, 4475936) and sequenced on an Ion Torrent Proton at the Saint Louis University Genomics Core Facility. Reads were aligned to the human genome hg19 assembly, and data are presented as total normalized nucleotide coverage per miRNA. Data on miR expression levels in human tissues was from the Human miRNA Tissue Atlas.[20]

Polysome profiling – H4 cells were cultured in 100-mm dishes and treated with 5 µM ASOs for 22 h. Five minutes prior to collecting cells, cycloheximide (CHX) was added to the cell culture media at a final concentration of 0.1 mg/ml. Cells were rinsed with ice-cold PBS, and then lysed in Polysome Lysis Buffer containing 20 mM Tris-HCl pH 7.4, 100 mM KCl, 5 mM $MgCl_2$, 1% NP-40, 0.1 mg/ml CHX, 1 mM DTT, 0.02 U/ml SUPERase In RNase Inhibitor (Invitorgen, AM2694),

protease inhibitors (Roche, cOmplete Mini EDTA-free Protease Inhibitor Cocktail), and phosphatase inhibitors (Roche, PhosSTOP) in nuclease-free water (Invitrogen, AM9937). Lysates were centrifuged (10,000 x g, 10 min, 4 °C), and the supernatant fractions were collected. Protein determination was performed using the Bio-Rad DC Protein Assay Kit II, and 1.35 mg per sample was loaded on a 15% to 45% sucrose density gradient (w/w sucrose, 20 mM Tris-HCl pH 7.4, 100 mM KCl, 5 mM $MgCl_2$, Ultrapure water). Samples were centrifuged for 2 h at 210,200 x g at 4 °C in a SW41 Ti rotor. Polysome profiling was performed using a BR-188 density gradient fractionation system (Brandel) (sensitivity setting of 1, baseline setting of 20, and flow rate of 1.5 ml/min) with upward displacement and continuous monitoring at 254 nm using a UA-6 detector. Polyribosome (13 fractions) and monosome (3 fractions) fractions were collected in a volume of 600 µl, and the fractions were separated in two tubes (300 µl per tube). For subsequent RNA extraction, 600 µl Trizol Reagent (Invitrogen, 15-596-018) was added to each polyribosome fraction (300 µl), and samples were stored at -80 ^{o}C. RNA was extracted by adding 200 µl chloroform (Fisher, C298) to each fraction and centrifuging at 18,213 x g for 15 min. The aqueous phase was transferred to a tube containing 500 µl of isopropanol (Fisher, A416P-4) and 5 µg of glycogen (Sigma, G1767-1VL). Then samples were pelleted at 18,213 x g for 15 min, dried, washed with 70% ethanol, and centrifuged at 18,213 x g for 15 min. The pellet was dried and resuspended in 20 µl of Ultrapure water. Samples were digested with DNase (Roche) for 40 min at 37 ^{o}C. cDNA was generated using 2 µg of RNA for each fraction with a High-Capacity cDNA Reverse Transcription Kit (ThermoFisher, 4368814). qPCR was performed using PowerUp SYBR Green Master Mix (ThermoFisher, A25776) using a QuantStudio 5 Real-Time PCR System. Primers sequences were as follows: human Actin-F, TCCGTGTGGATCGGCGGCTCCA; human Actin-R, CTGCTTGCTGATCCACATCTG; human GRN-F, AGGAGAACGCTACCACGGA; and human GRN-R, GGCAGCAGGTATAGCCATCTG. Relative RNA levels were calculated using a C_t mean value normalized with an internal control (Actin). The delta C_T value is then normalized to the delta C_T value of the input (taken before the polyribosome profiling) from the corresponding condition.

AHA labeling – H4 cells were cultured in DMEM high glucose (Gibco, 11965-092) supplemented with 10% FBS (Gibco, 10010-023). Cells were cultured in 60-mm plate until about 80% confluence and treated with 10 µM ASOs for a total of 24 h. For optimal incorporation of the amino acid azidohomoalanine (AHA), cells were methionine-deprived for 2.5 h in methionine-free medium (DMEM without methionine, glutamine, and cysteine (Gibco, 21013024), supplemented with 0.5% FBS, 1X GlutaMAX (Gibco, 35050061), and 63 µg/ml L-Cysteine) containing 10 µM ASO. AHA was then added to the cell culture medium at a final concentration of 50 µM for the last 2 h of treatment to label de novo proteins. Cells were washed once with ice-cold PBS containing 0.1 mg/ml CHX, and then lysed in Triton lysis buffer containing 1% Triton X-100, 25 mM sodium pyrophosphate, 150 mM NaCl, 50 mM NaF, 5 mM EDTA, 5mM EGTA, 0.5% sodium deoxycholate, 20 mM HEPES pH 7.4, 10 mM β-glycerophosphate, 1 mM Na_3VO_4, 0.1 mg/ml CHX, and protease inhibitors (Roche, cOmplete Mini EDTA-free Protease Inhibitor Cocktail). Lysates were centrifuged (16,260 x g, 10 min, 4 °C), and the supernatant fractions were collected. Click reactions were performed using Click-iT Protein Reaction Buffer Kit (Invitrogen, C10276) according to the manufacturer's protocol in order to label the AHA-incorporated proteins with biotin alkyne (ThermoFisher,

B10185). The Click reaction samples were incubated on a rotator at 4 °C for 1 h, and diluted in lysis buffer at a 1:2 ratio before being subjected to anti-progranulin immunoprecipitation. For immunoprecipitation, the lysates were incubated with rotation with 8.4 µg of anti-human progranulin linker 4 polyclonal antibody #611 (which recognizes an epitope between amino acids 422–440)[27] overnight at 4 °C, followed by a 2 h incubation with Protein A Agarose beads (Roche, 11719408001) at 4 °C. Beads were washed three times with the lysis buffer and the immunoprecipitates were eluted, denatured and boiled (5 min, 95 °C) in 2X Laemmli buffer. For western blot analysis, the immunoprecipitated samples were resolved on 10% SDS–PAGE gels, transferred to nitrocellulose membranes, and stained with Ponceau. After blocking incubations, the membranes were incubated with IRDye 800CW Streptavidin (LICOR, 926-32230) to detect AHA-labelled proteins with the LICOR Odyssey imaging system. The membrane was reprobed with anti-human progranulin linker 5 polyclonal antibody #614 (1:3000) using Quick Western Kit-IRDye 680RD secondary antibody (LICOR, PN 926-69100).

MTT assay – MTT assays were used to assess the effects of ASOs on cell viability. H4 cells were plated in 96-well plates at a density of 5,000 cells per well. The following day, cell were treated with 10 µM ASO. After 21 h treatment, the media was removed and cells were incubated in 100 µl of 0.5 mg/ml thiazolyl blue tetrazolium bromide (MTT) (Sigma, M5655) solution prepared in fresh culture media for 4 h. After incubation, the MTT solution was removed and 100 µl of DMSO was added to dissolve the crystals formed. The absorbance was measured at 570 nm using a BioTek Synergy H1 plate reader. Experiments were performed with triplicate wells, and the percent viability was normalized to cells treated with vehicle only (water).

FRET-based assay for miR-29b binding – A FRET-based assay was developed to monitor the interaction between miR-29b (labeled with Cy3 at the 5' end) and a partial *GRN* 3' UTR RNA (nucleotides 189–246, labeled with Cy5 at the 3' end). Reactions were set up in duplicate wells in black 384-well plates with 1 µM miR-29b and 1 µM *GRN* 3' UTR in 20 µl of 1X SSC buffer, pH 7.0 containing 0.005% Tween-20. ASOs were added to the reactions in the same buffer at final concentrations between 0.64 nM–50 µM. Plates were read using a BioTek Synergy H1 plate reader with excitation at 540 nm and emission at 570 nm, and with excitation at 540 nm and emission at 665 nm. The ratio of fluorescence emissions at 665 nm / 570 nm was calculated for each well, and data were transformed with baseline correction.

Mouse studies – Animal procedures were approved by the Institutional Animal Care and Use Committee of Saint Louis University and followed NIH guidelines. Mice were housed in a pathogen-free barrier facility with a 12-h light/12-h dark cycle and provided food and water ad libitum. Humanized *GRN* mice[22] were on the C57BL/6J background and were genotyped either by PCR as described[22] or by real-time PCR (Transnetyx). For ASO delivery, 500 µg ASO (in 5 µl PBS) was administered by intracerebroventricular (ICV) injection into the right lateral ventricle of mice anesthetized with isoflurane, as previously described.[28] After 3 weeks, mice were sacrificed and brain tissues were collected for protein analysis. For ELISA, progranulin levels were determined in duplicate using 150 µg of protein lysates per well using a sandwich ELISA assay (abcam, ab252364). Western blots were carried out as described above.

Statistical analyses – Data are presented as means ± SD or as means ± SEM, as indicated in the figure legends. Data were analyzed with GraphPad Prism software (GraphPad) using the statistical tests described in the figure legends. P values < 0.05 were considered significant.

DATA AVAILABILITY

The RNA-seq dataset has been deposited in the Gene Expression Omnibus (GEO) under accession number GSE188498.

ACKNOWLEDGEMENTS

We thank Michael Ward for providing iPSCs for differentiation into i3 neurons, the Genomics Core Facility at Saint Louis University for RNA-seq, Sophie Chang for technical assistance, and Laura Mitic for helpful discussions. This work was supported by grants from the NIH (AG064069), NIH/National Center for Advancing Translational Sciences (NCATS) (UL1TR002345), Bluefield Project to Cure FTD, Natural Sciences and Engineering Research Council of Canada (NSERC, RGPIN-2018-06227, RGPIN-2020-06376, DGECR-2018-00093, and DGECR-2020-00060), Brain Canada Future Leaders Grant, and Fonds de Recherche du Québec Santé Junior-1.

DECLARATION OF INTERESTS

K.L., P.J.-N., and F.R. are paid employees of Ionis Pharmaceuticals. Saint Louis University has filed for a patent based on using *GRN* ASOs to treat frontotemporal dementia. The authors declare no other competing financial interests.

FIGURE LEGENDS

Figure 1. ASOs targeting the miR-29 binding site in the human *GRN* mRNA increase progranulin protein levels. (**a**) ELISA for progranulin protein levels in H4 neuroglioma cells following treatment with miR-29b inhibitor for 24 h. (**b**) Schematic of the *GRN* 3' UTR indicating miR binding sites and region targeted by ASOs. (**c**) Western blot validation of candidate ASOs in H4 cells (10 µM, 24 h). (**d**) Dose curve of ASO treatment in H4 cells (24 h), as determined by ELISA. (**e**) Western blot of progranulin in iPSC-derived neurons following ASO treatment at the indicated concentrations (µM) (3–4 d). (**f**-**g**) Human progranulin levels in brains of humanized *GRN* mice at 3 weeks after ICV administration of 500 µg ASO. (**f**) Human progranulin levels in cortex, as determined by ELISA. (**g**) Western blot of human progranulin in cortex, thalamus, and hippocampus. Data are presented as means ± SD in (**a**) and (**d**) or as means ± SEM in (**f**); * indicates p<0.05 and ** indicates p<0.01, as determined by one-way ANOVA with Dunnett post hoc test. Non-Tg, non-transgenic.

Figure 2. ASOs increase progranulin translation by displacing miR-29b binding. (**a**) *GRN* mRNA levels following ASO treatment (5 µM, 24 h), as determined by qPCR. (**b**) *GRN* mRNA distribution in each of 16 sucrose gradient fractions from ASO-treated H4 cells (5 µM, 22 h) analyzed by qPCR. Fraction 1: hydrosoluble fraction; fractions 2, 3, and 4: 40S, 60S, and monosomes, respectively; fractions 5–10: light polyribosomes; and fractions 11–16: heavy polyribosomes. Data are plotted as a fraction of total mRNA on the gradient. (**c**) Western blot showing immunoprecipated, newly synthesized, AHA/biotin-labeled progranulin protein following ASO treatment (10 µM, 24 h). (**d**) ELISA for progranulin protein levels after co-treatment with miR-29b inhibitor (70 µM) and ASOs (20 µM) for 24 h. (**e**) FRET assay demonstrating multiple ASOs can compete miR-29b from binding to a partial *GRN* 3' UTR RNA. Data are presented as means ± SD; * indicates $p<0.05$, ** indicates $p<0.01$, and *** indicates $p<0.001$ as determined by one-way ANOVA with Dunnett post hoc test in (**a**) and (**c**), and by two-way ANOVA with Tukey post hoc test in (**d**). PGRN, progranulin; n.s., not significant.

Supplementary Figure S1. miR-29b is moderately expressed in human H4 neuroglioma cells and in the human brain. (**a**) Ranked profile of miR expression levels in H4 cells, as determined by RNA-seq. miR-29b is indicated in red.(**b**) Expression levels of miRs known to regulate progranulin levels in the human brain. Data from the Human miRNA Tissue Atlas.[22]

Supplementary Figure S2. Validation of ASO hits from initial screening. H4 cells were treated with 5 µM ASO for 24 h, and progranulin levels were measured in cell lysates by ELISA. Data are presented as means ± SD; * indicates $p<0.05$, ** indicates $p<0.01$, *** indicates $p<0.001$, and **** indicates $p<0.0001$, as determined by one-way ANOVA with Dunnett post hoc test.

Supplementary Figure S3. ASOs increase both cellular and secreted progranulin levels. After treatment with 10 µM ASO for 24 h, progranulin levels in cell lysates and in the conditioned media were determined by western blot.

Supplementary Figure S4. Time course of ASO treatment. H4 cells were treated with 10 µM ASO for the indicated times, and progranulin levels in cell lysates were determined by western blot.

Supplementary Figure S5. Dose curves of selected ASOs. H4 cells were treated with ASO for 24 h, and progranulin levels were measured in cell lysates by ELISA. Data are presented as means ± SD, with EC_{50} values indicated.

Supplementary Figure S6. ASOs are not toxic in cells. H4 cells were treated with 10 µM ASO for 21 h, and subsequently cell viability was assessed by MTT assay. Data are presented as means ± SD.

Supplementary Figure S7. Several ASOs targeting the miR-659 binding site in the *GRN* 3' UTR increase progranulin protein levels. H4 cells were treated with 5 µM ASO for 24 h, and progranulin levels were measured in cell lysates by ELISA. Data are presented as means ± SD; * indicates $p<0.05$ and *** indicates $p<0.001$, as determined by one-way ANOVA with Dunnett post hoc test.

REFERENCES

1. Cruts M, Gijselinck I, van der Zee J, et al. Null mutations in progranulin cause ubiquitin-positive frontotemporal dementia linked to chromosome 17q21. *Nature.* 2006;442(7105):920-924.

2. Baker M, Mackenzie IR, Pickering-Brown SM, et al. Mutations in progranulin cause tau-negative frontotemporal dementia linked to chromosome 17. *Nature.* 2006;442(7105):916-919.

3. Schoch KM, Miller TM. Antisense oligonucleotides: Translation from mouse models to human neurodegenerative diseases. *Neuron.* 2017;94(6):1056-1070.

4. Leavitt BR, Tabrizi SJ. Antisense oligonucleotides for neurodegeneration. *Science.* 2020;367(6485):1428-1429.

5. Kao AW, McKay A, Singh PP, Brunet A, Huang EJ. Progranulin, lysosomal regulation and neurodegenerative disease. *Nat Rev Neurosci.* 2017;18(6):325-333.

6. Paushter DH, Du H, Feng T, Hu F. The lysosomal function of progranulin, a guardian against neurodegeneration. *Acta Neuropathol.* 2018;136(1):1-17.

7. Terryn J, Verfaillie CM, Van Damme P. Tweaking progranulin expression: therapeutic avenues and opportunities. *Front Mol Neurosci.* 2021;14:713031.

8. Amin S, Carling G, Gan L. New insights and therapeutic opportunities for progranulin-deficient frontotemporal dementia. *Curr Opin Neurobiol.* 2021;72:131-139.

9. Arrant AE, Filiano AJ, Unger DE, Young AH, Roberson ED. Restoring neuronal progranulin reverses deficits in a mouse model of frontotemporal dementia. *Brain.* 2017;140(5):1447-1465.

10. Liang XH, Shen W, Sun H, Migawa MT, Vickers TA, Crooke ST. Translation efficiency of mRNAs is increased by antisense oligonucleotides targeting upstream open reading frames. *Nat Biotechnol.* 2016;34(8):875-880.

11. Liang XH, Sun H, Shen W, et al. Antisense oligonucleotides targeting translation inhibitory elements in 5' UTRs can selectively increase protein levels. *Nucleic Acids Res.* 2017;45(16):9528-9546.

12. Lewis BP, Burge CB, Bartel DP. Conserved seed pairing, often flanked by adenosines, indicates that thousands of human genes are microRNA targets. *Cell.* 2005;120(1):15-20.

13. Friedman RC, Farh KK, Burge CB, Bartel DP. Most mammalian mRNAs are conserved targets of microRNAs. *Genome Res.* 2009;19(1):92-105.

14. Iwakawa HO, Tomari Y. The functions of microRNAs: mRNA decay and translational repression. *Trends Cell Biol.* 2015;25(11):651-665.

15. Jiao J, Herl LD, Farese RV, Gao FB. MicroRNA-29b regulates the expression level of human progranulin, a secreted glycoprotein implicated in frontotemporal dementia. *PLoS One.* 2010;5(5):e10551.

16. Chen L, Li Q, Wang J, et al. MiR-29b-3p promotes chondrocyte apoptosis and facilitates the occurrence and development of osteoarthritis by targeting PGRN. *J Cell Mol Med.* 2017;21(12):3347-3359.

17. Rademakers R, Eriksen JL, Baker M, et al. Common variation in the miR-659 binding-site of GRN is a major risk factor for TDP43-positive frontotemporal dementia. *Hum Mol Genet.* 2008;17(23):3631-3642.

18. Piscopo P, Grasso M, Fontana F, et al. Reduced miR-659-3p levels correlate with progranulin increase in hypoxic conditions: implications for frontotemporal dementia. *Front Mol Neurosci.* 2016;9:31.

19. Wang WX, Wilfred BR, Madathil SK, et al. miR-107 regulates granulin/progranulin with implications for traumatic brain injury and neurodegenerative disease. *Am J Pathol.* 2010;177(1):334-345.

20. Ludwig N, Leidinger P, Becker K, et al. Distribution of miRNA expression across human tissues. *Nucleic Acids Res.* 2016;44(8):3865-3877.

21. Fernandopulle MS, Prestil R, Grunseich C, Wang C, Gan L, Ward ME. Transcription factor-mediated differentiation of human iPSCs into neurons. *Curr Protoc Cell Biol.* 2018;79(1):e51.

22. Petkau TL, Life B, Lu G, et al. Human progranulin-expressing mice as a novel tool for the development of progranulin-modulating therapeutics. *Neurobiol Dis.* 2021;153:105314.

23. Jafar-Nejad P, Powers B, Soriano A, et al. The atlas of RNase H antisense oligonucleotide distribution and activity in the CNS of rodents and non-human primates following central administration. *Nucleic Acids Res.* 2021;49(2):657-673.

24. O'Brien J, Hayder H, Zayed Y, Peng C. Overview of microRNA biogenesis, mechanisms of actions, and circulation. *Front Endocrinol.* 2018;9:402.

25. Choi WY, Giraldez AJ, Schier AF. Target protectors reveal dampening and balancing of Nodal agonist and antagonist by miR-430. *Science.* 2007;318(5848):271-274.

26. Viart V, Bergougnoux A, Bonini J, et al. Transcription factors and miRNAs that regulate fetal to adult CFTR expression change are new targets for cystic fibrosis. *Eur Respir J.* 2015;45(1):116-128.

27. Nguyen AD, Nguyen TA, Cenik B, et al. Secreted progranulin is a homodimer and is not a component of high density lipoproteins (HDL). *J Biol Chem.* 2013;288(12):8627-8635.

28. Farr SA, Erickson MA, Niehoff ML, Banks WA, Morley JE. Central and peripheral administration of antisense oligonucleotide targeting amyloid-β protein precursor improves learning and memory and reduces neuroinflammatory cytokines in Tg2576 (AβPPswe) mice. *J Alzheimers Dis.* 2014;40(4):1005-1016.

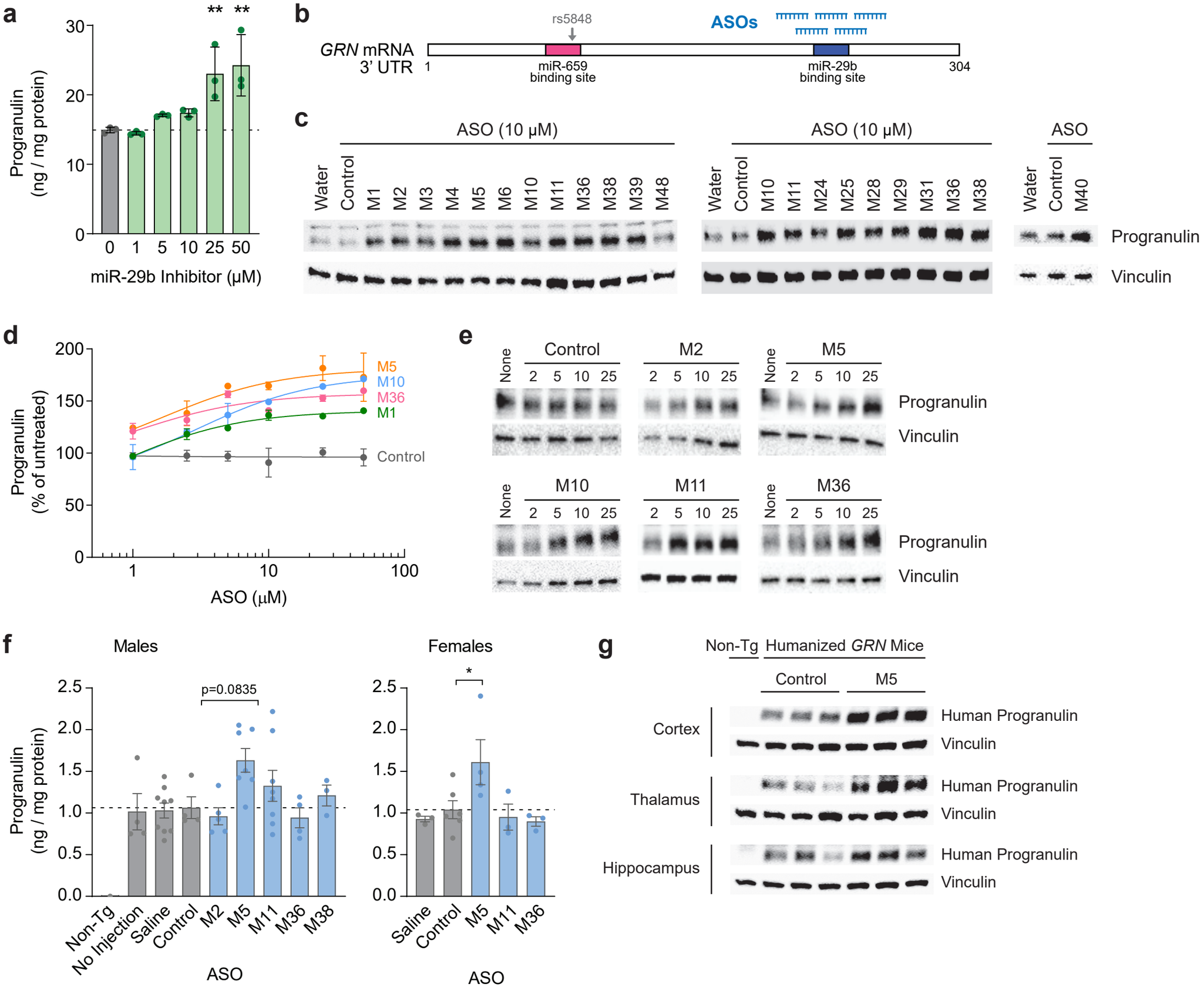
a
Progranulin (ng / mg protein)
miR-29b Inhibitor (μM)
0 1 5 10 25 50
** **
b
rs5848
ASOs
GRN mRNA 3' UTR
1
304
miR-659 binding site
miR-29b binding site
c
ASO (10 μM)
Water Control M1 M2 M3 M4 M5 M6 M10 M11 M36 M38 M39 M48
Water Control M10 M11 M24 M25 M28 M29 M31 M36 M38
ASO
Water Control M40
Progranulin
Vinculin
d
Progranulin (% of untreated)
ASO (μM)
M5
M10
M36
M1
Control
e
None
Control
M2
M5
M10
M11
M36
2 5 10 25
Progranulin
Vinculin
f
Males
Females
Progranulin (ng / mg protein)
p=0.0835
*
Non-Tg
No Injection
Saline
Control
M2
M5
M11
M36
M38
ASO
g
Non-Tg
Humanized GRN Mice
Control
M5
Cortex
Thalamus
Hippocampus
Human Progranulin
Vinculin

Figure 1

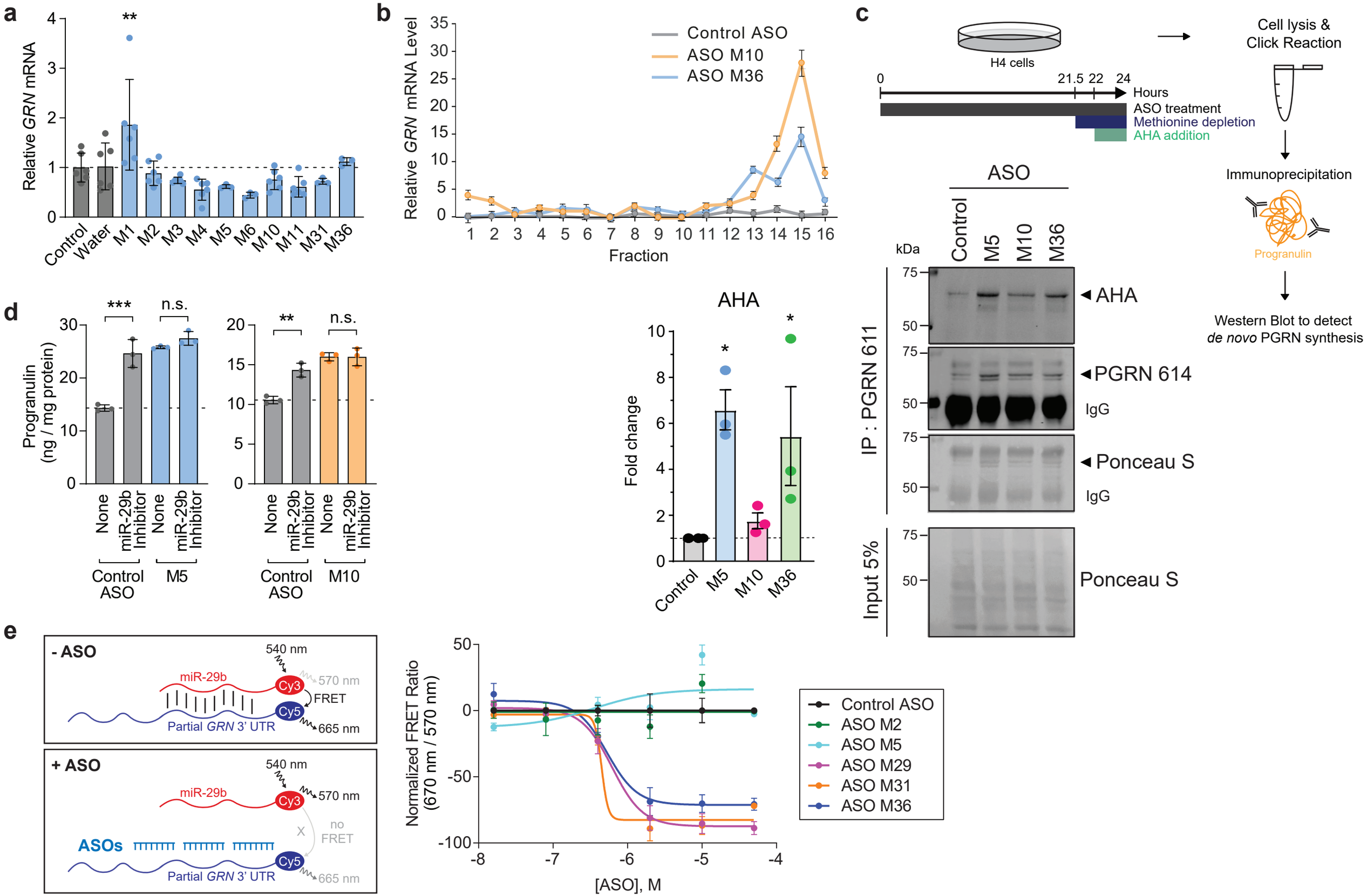
a
Relative GRN mRNA
**
Control
Water
M1
M2
M3
M4
M5
M6
M10
M11
M31
M36
b
Relative GRN mRNA Level
Control ASO
ASO M10
ASO M36
Fraction
c
H4 cells
Cell lysis & Click Reaction
0
21.5
22
24
Hours
ASO treatment
Methionine depletion
AHA addition
Immunoprecipitation
Progranulin
Western Blot to detect de novo PGRN synthesis
ASO
Control
M5
M10
M36
kDa
AHA
PGRN 614
IgG
Ponceau S
IgG
IP : PGRN 611
Input 5%
Ponceau S
d
Progranulin (ng / mg protein)
***
n.s.
**
n.s.
None
miR-29b Inhibitor
Control ASO
M5
M10
AHA
Fold change
*
*
Control
M5
M10
M36
e
- ASO
540 nm
miR-29b
Cy3
570 nm
FRET
Cy5
665 nm
Partial GRN 3' UTR
+ ASO
ASOs
X
no FRET
Normalized FRET Ratio (670 nm / 570 nm)
[ASO], M
Control ASO
ASO M2
ASO M5
ASO M29
ASO M31
ASO M36

Figure 2

a

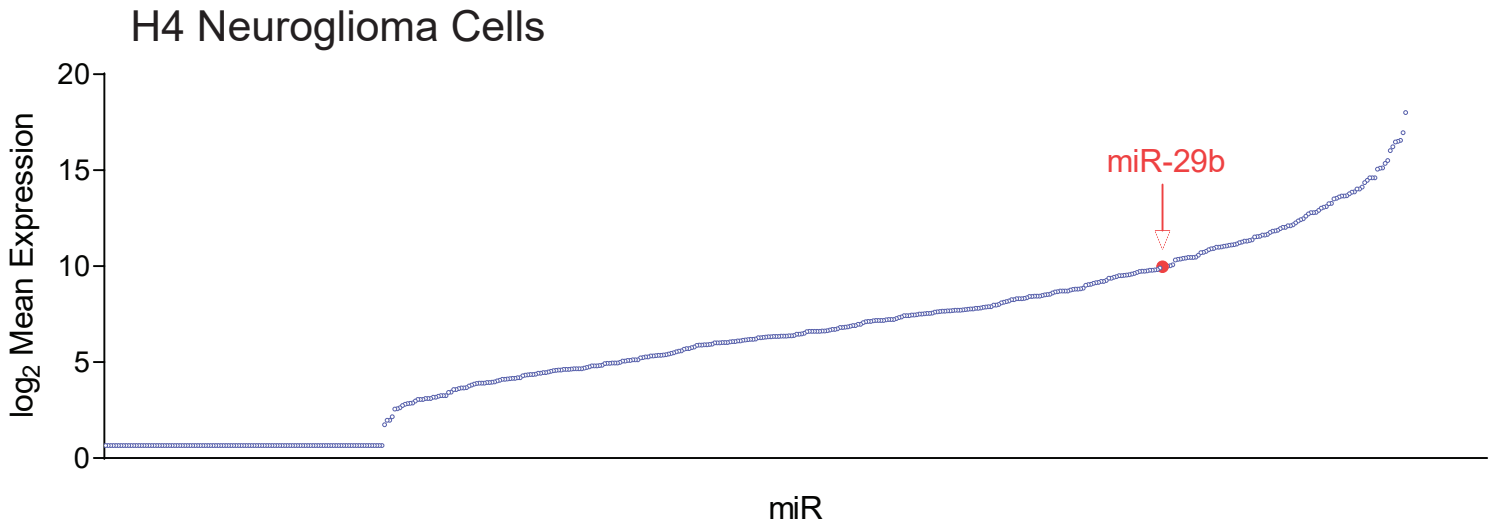

b

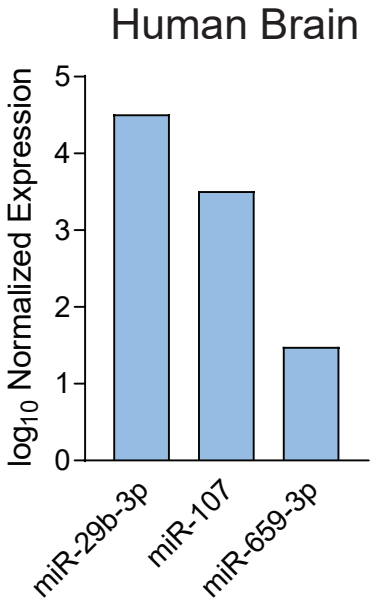

Supplementary Figure S1

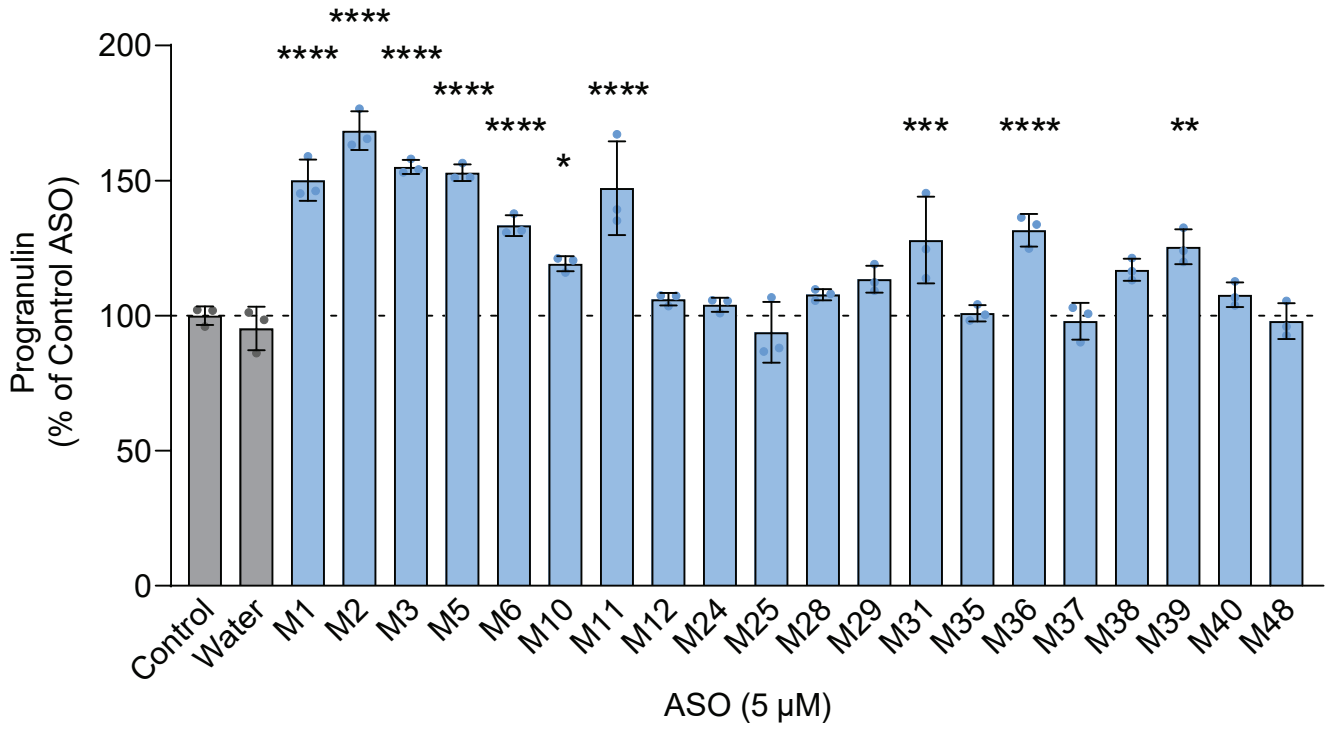

Supplementary Figure S2

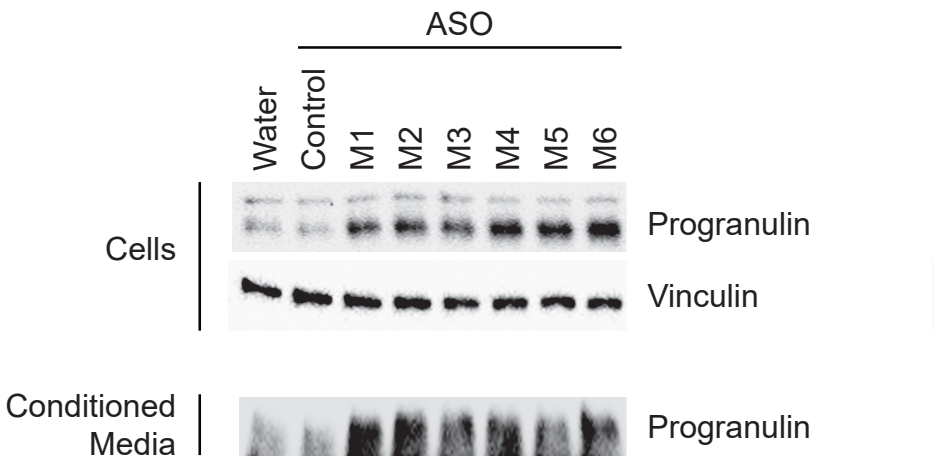

Supplementary Figure S3

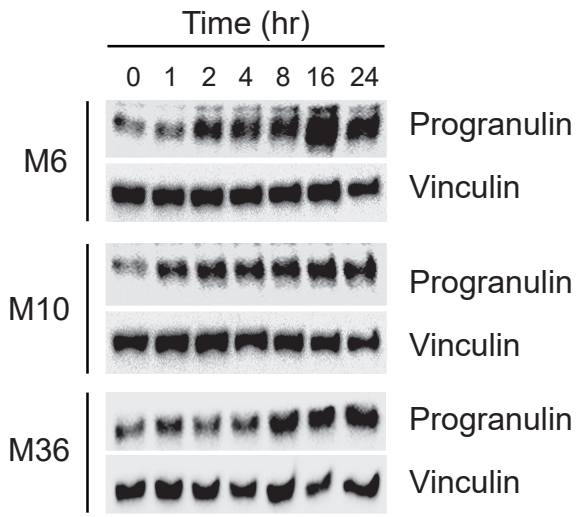

Supplementary Figure S4

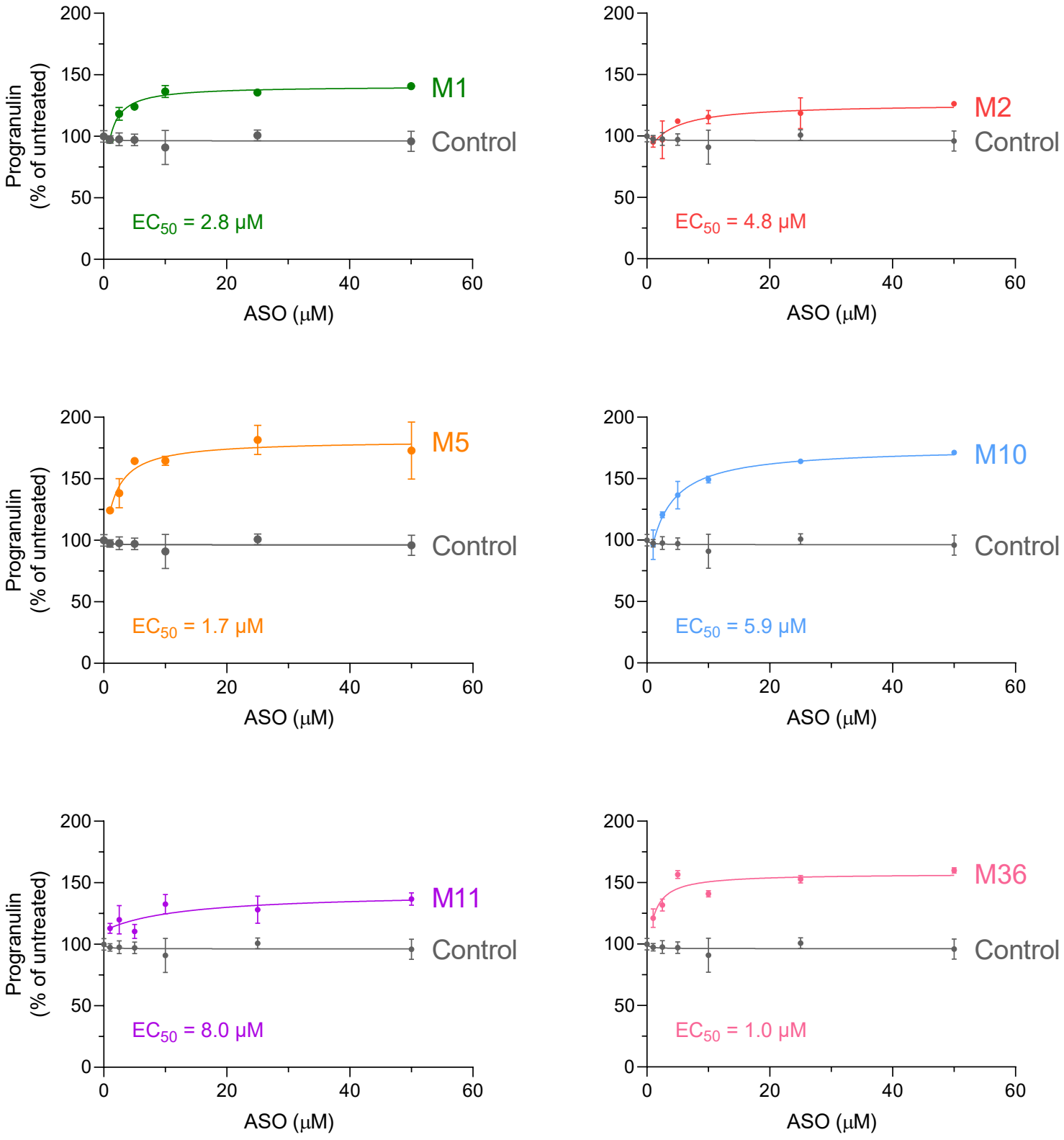

Supplementary Figure S5

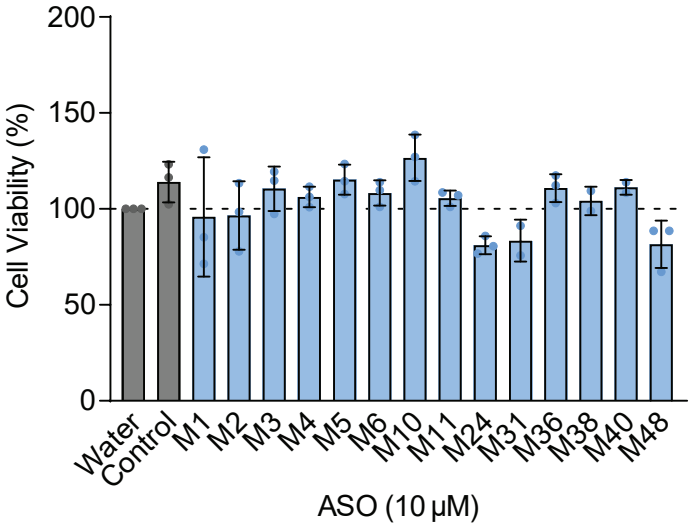

Supplementary Figure S6

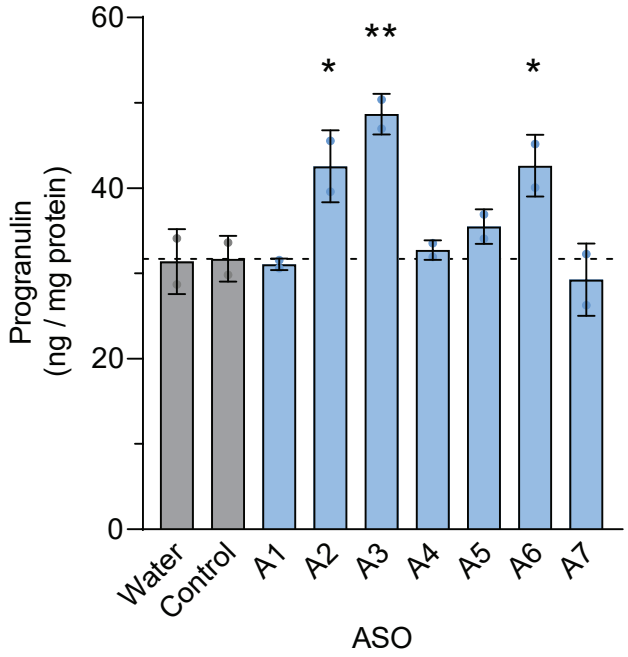

Supplementary Figure S7